Kinetic adaptation during locomotion on a split-belt treadmill

Firas Mawase, Tamar Haizler, Simona Bar-Haim and Amir Karniel

You might find this additional info useful...

This article cites 71 articles, 35 of which you can access for free at:
http://jn.physiology.org/content/109/8/2216.full#ref-list-1

Updated information and services including high resolution figures, can be found at:
http://jn.physiology.org/content/109/8/2216.full

Additional material and information about *Journal of Neurophysiology* can be found at:
http://www.the-aps.org/publications/jn

This information is current as of May 29, 2013.

Kinetic adaptation during locomotion on a split-belt treadmill

Firas Mawase,[1,3] Tamar Haizler,[1] Simona Bar-Haim,[2,3] and Amir Karniel[1,3]

[1]*Department of Biomedical Engineering, Ben-Gurion University of the Negev, Beer-Sheva, Israel;* [2]*Department of Physiotherapy, Ben-Gurion University of the Negev, Beer-Sheva, Israel; and* [3]*Zlotowski Center for Neuroscience, Ben-Gurion University of the Negev, Beer-Sheva, Israel*

Mawase F, Haizler T, Bar-Haim S, Karniel A. Kinetic adaptation during locomotion on a split-belt treadmill. *J Neurophysiol* 109: 2216–2227, 2013. First published January 30, 2013; doi:10.1152/jn.00938.2012.—It has been suggested that a feedforward control mechanism drives the adaptation of the spatial and temporal interlimb locomotion variables. However, the internal representation of limb kinetics during split-belt locomotion has not yet been studied. In hand movements, it has been suggested that kinetic and kinematic parameters are controlled by separate neural processes; therefore, it is possible that separate neural processes are responsible for kinetic and kinematic locomotion parameters. In the present study, we assessed the adaptation of the limb kinetics by analyzing the ground reaction forces (GRFs) as well as the center of pressure (COP) during adaptation to speed perturbation, using a split-belt treadmill with an integrated force plate. We found that both the GRF of each leg at initial contact and the COP changed gradually and showed motor aftereffects during early postadaptation, suggesting the use of a feedforward predictive mechanism. However, the GRF of each leg in the single-support period used a feedback control mechanism. It changed rapidly during the adaptation phase and showed no motor aftereffect when the speed perturbation was removed. Finally, we found that the motor adaptation of the GRF and the COP are mediated by a dual-rate process. Our results suggest two important contributions to neural control of locomotion. First, different control mechanisms are responsible for forces at single- and double-support periods, as previously reported for kinematic variables. Second, our results suggest that motor adaptation during split-belt locomotion is mediated by fast and slow adaptation processes.

internal model; limb kinetics; ground reaction force; split-belt adaptation; locomotion

THE HUMAN BRAIN HAS DEVELOPED an exceptional ability to adapt and to learn novel motor tasks. It has been suggested that this ability was achieved by creating internal models of the environmental dynamics (Emken and Reinkensmeyer 2005; Kawato 1999; Thoroughman and Shadmehr 2000; Wolpert et al. 1995), internal models that facilitate the generation of motor commands and are updated according to the motor errors caused by unexpected environment perturbation. Extensive studies have examined the adaptation to different novel motor tasks such as reaching movements in force field perturbation (Donchin et al. 2003; Scheidt et al. 2000; Shadmehr and Mussa-Ivaldi 1994; Smith et al. 2006), reaching with visuomotor rotation (Krakauer et al. 2000; Mazzoni and Krakauer 2006; Peled and Karniel 2012), grasping movements with load perturbation (Flanagan and Rao 1995; Flanagan and Wing 1997; Mawase and Karniel 2010), and locomotor adaptation to a split-belt treadmill (Reisman et al. 2005, 2007). Similar

phenomena of adaptation and aftereffect have been shown in several previous studies of human locomotion. Investigations examined the process of motor adaptation to external force field perturbations during walking by manipulation of the mechanical properties of the limbs that involved adding and removing external load (Noble and Prentice 2006), by applying elastic resistance to the limbs during walking (Blanchette et al. 2012; Fortin et al. 2009), and by using a novel exoskeleton robot attached to the legs (Gordon and Ferris 2007; Kao and Ferris 2009). All of these studies found evidence for the presence of motor aftereffects during the postadaptation period when analyzing the muscle activation pattern, angular moments, as well as many kinematic data.

In our everyday activities we have adapted our walking pattern for different changes in the environment (Choi et al. 2009). To study how the limb kinematics changes during split-belt locomotion, which limb parameters change immediately with feedback control, and which limb parameters are stored and show aftereffect with feedforward control, Reisman et al. (2005) examined the adaptation of the interlimb and intralimb spatial and temporal parameters during adaptation to split-belt locomotion. The split-belt treadmill allows control of each belt speed independently and perturbation of the locomotion pattern. They found that subjects immediately changed intralimb spatial and temporal parameters (stride length and single-support time) as a reaction to the split-belt perturbations. However, interlimb spatial and temporal parameters (step length and double-support time) changed slowly and showed clear aftereffects in early postadaptation. These novel and interesting results paved the way to many recent studies aimed at understanding the brain functionality of the lower limb kinematic behavior during interaction with split-belt speed perturbations in unimpaired subjects (Tesio and Rota 2008; Vasudevan and Bastian 2010; Yang et al. 2005) as well as in cerebellar and cerebral patients (Choi et al. 2009; Morton and Bastian 2006; Reisman et al. 2007). However, the limb kinetic behavior during such adaptation was not measured and analyzed in the previous studies.

Knowledge about limb kinetic and kinematic changes (i.e., errors) is essential for understanding the neural control of movement. Although both types of error appear during motor adaptation, they might affect the control of the limbs differently. In the motor control literature, there are various observations concerning motor behavior and neural control of kinetics- and kinematics-driven adaptation. On one hand, Kao et al. (2010) proposed that the motor system minimizing the kinetic error (e.g., joint moments) during locomotor adaptation to a robotic exoskeleton, suggesting that kinetic error drives motor adaptation. On the other hand, Reisman et al. (2005)

proposed that kinematic error drives locomotor adaptation by minimizing the step symmetry during walking on a split-belt treadmill. Furthermore, recent neuroimage and brain stimulation studies have emphasized this point of interesting dispute. Chib et al. (2009) used transcranial magnetic stimulation (TMS) to study the involvement of parietal regions of the cerebral cortex in force and position control. They found that control of hand movements and contact forces while manipulating objects is performed by an independent neural control process. However, Diedrichsen et al. (2005) used fMRI technique and suggested that kinematic and dynamic errors during reach movements are performed in one anatomically overlapped cerebellum area. To conclude, although it is certain that kinematic (e.g., step length, double-support time, etc.) and kinetic [e.g., ground reaction forces (GRFs), center of pressure (COP), etc.] parameters are correlated during locomotor adaptation, it remains to be determined whether the motor system controls these parameters by shared adaptive process or alternatively by separate processes. To this end, we tested how kinetic parameters (GRFs and COPs) change during adaptation to a split-belt force treadmill and whether these parameters adapt in a similar or different way as kinematic parameters as previously shown (Reisman et al. 2005). Finally, we discuss the implications of these results for our understanding of locomotion neural control.

MATERIALS AND METHODS

Subjects. Ten healthy subjects [6 men, 4 women, mean age 25.8 ± 3.4 (SD) yr] without a neurological history and without known disturbances in walking participated in this study. The dominant leg of all subjects was the right leg. Leg dominance was determined by asking each subject about the leg he/she uses to kick a ball. All subjects signed the informed consent form as stipulated by the Institutional Helsinki Committee, which reviewed and approved all protocols.

Setup and experimental protocol. Subjects were instructed to walk on a custom split-belt force treadmill (ForceLink, Clemborg, The Netherlands) that has two separate belts and an embedded force plate underneath (Fig. 1A). The speed of each treadmill belt was controlled independently by its own motor. During the experiment, subjects walked on the split-belt force treadmill while the belts' speed could be in one of two conditions, either moved together at similar speeds or moved separately at different speeds. The force plate was located under the split-belt treadmill as validated by Tesio and Rota (2008).

The protocol applied in the present study was similar to those used in previous studies on locomotion control (Morton and Bastian 2006; Reisman et al. 2005, 2007). The experiment was divided into three phases: baseline, adaptation, and postadaptation (Reisman et al. 2005). During the baseline phase, subjects walked with both belts at "slow" speed, then at "fast" speed, and finally at "slow" speed for 2 min at each speed. We define "slow" and "fast" speeds to be 0.5 m/s and 1 m/s, respectively. We chose these speed levels for two reasons. First, to compare our kinetic results with previous studies in kinematic adaptation, we chose levels similar to those described previously (Morton and Bastian 2006; Reisman et al. 2005, 2007). Second, the chosen speed levels were within the range of the self-paced walking speed in healthy subjects (Cunningham et al. 1982). The self-paced speed is known as a natural speed of stable and comfortable walking. During adaptation, subjects walked with the belts of the split-belt force treadmill moving at different speeds for 15 min; the subject's left (nondominant) leg always walked in the slow speed condition, while the right (dominant) leg walked in the fast speed condition. During postadaptation, the belts were set to move together in the slow speed condition (0.5 m/s) for 5 min (Fig. 1B). The purpose of the initial exposure (baseline periods) was to train subjects for the two levels of speed before the adaptation period and to evaluate the baseline level of GRF for calculating the GRF change acquired in the adaptation period. At the end of each phase, the treadmill stopped completely and a 5-s break was made for resetting the treadmill belt speeds. Subjects were instructed not to look down at the belts during the experiment, and we therefore carefully prevented the use of available visual feedback from the environment regarding the speeds of the belts. For safety, two emergency stop buttons were available
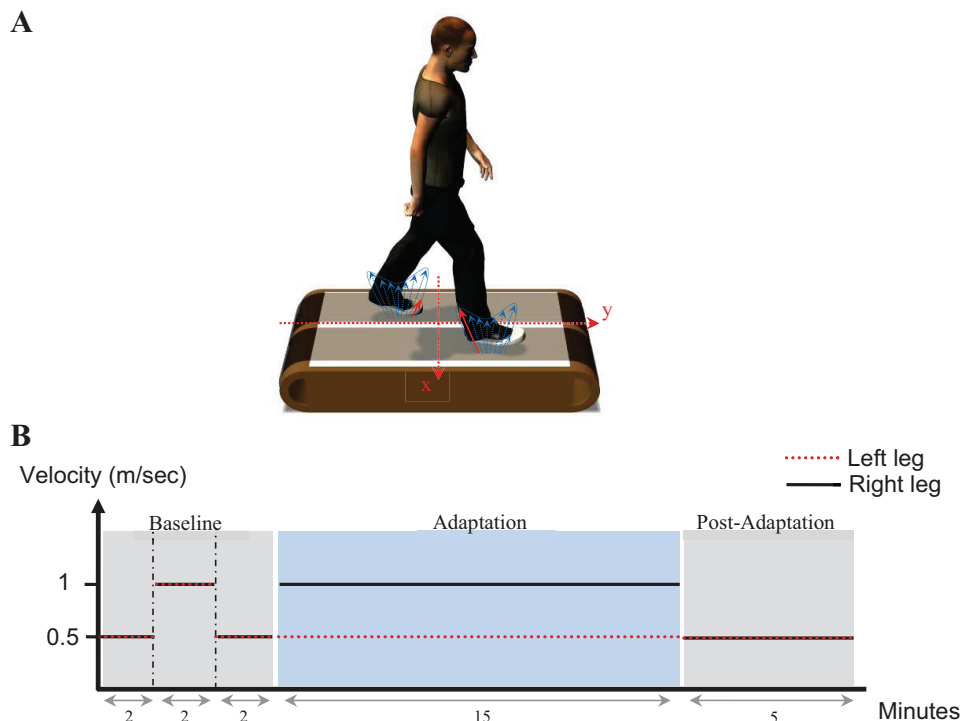
A

B

Fig. 1. Experiment setup and protocol. *A*: subjects were instructed to walk on a split-belt force treadmill that has 2 separated belts and an embedded force plate (white plate). Blue vectors for each leg illustrate the vertical ground force during stance phase. The red vector of the left leg illustrates the vertical ground reaction force (GRF) at left toe-off while the red vector of the right foot illustrates the force at foot contact. *B*: experimental protocol: slow baseline (2 min), fast baseline (2 min), slow baseline (2 min), adaptation (15 min), and postadaptation (5 min) phases. *y*-Coordinates are the speed of the belts in each phase (solid black and dashed red for right and left belts, respectively).

during the experiment and two adjustable side bars were available to prevent falls but did not support body weight. Custom software written in C# (Microsoft Visual Studio) was used for controlling the speed of the belts and the duration of the breaks during the experiment.

Data collection. GRF and COP were sampled and recorded with Gaitfors software (ForceLink). The system recorded the forces with one-dimensional force sensors from a single large (160 × 800 mm) force plate embedded in the treadmill. Force data were collected at 500 Hz. The system was also able to determine kinematic data and representative gait events such as initial contact (IC), toe-off (TO), and midstance (MS) for each leg independently. (For more details see Roerdink et al. 2008.) We define the coordinates of the split-belt movements as vertical movements in the *z*-direction, anterior-posterior movements in the *y*-direction, and lateral movements in the *x*-direction (Fig. 1*A*); therefore the one-dimensional force sensors recorded only the vertical forces (F_z). COP was measured as the point placement of the vertical GRF vector. It represents a weighted average

of the pressures all over the force plate of the area in contact with the ground.

Data analysis. Force data were low-pass filtered at 30 Hz (with a 4th-order Butterworth filter). Our analysis was based on measurement of the vertical GRF profiles that subjects generated during different states of locomotion. Since we were interested in determining whether GRF changes with a predictive feedforward or feedback mechanism, we calculated the GRF in double-limb support as well as in single-limb support. The forces of each subject were then normalized to his/her own body weight, preventing the effect of the variability of different weights in this measurement. Peaks of vertical GRF during double-limb support and single-limb support—maximum force in double support and minimal force in single support (Fig. 2*A*)—were chosen as representative points because of their importance in gait analysis (Cavanagh and Lafortune 1980; Munro et al. 1987). The peak of the GRF in double-limb support was analyzed as the maximal force point that occurs immediately after left initial contact (LIC) or right initial contact (RIC), whereas the peak of the GRF in single-limb support was analyzed as the minimal force point that occurs imme-
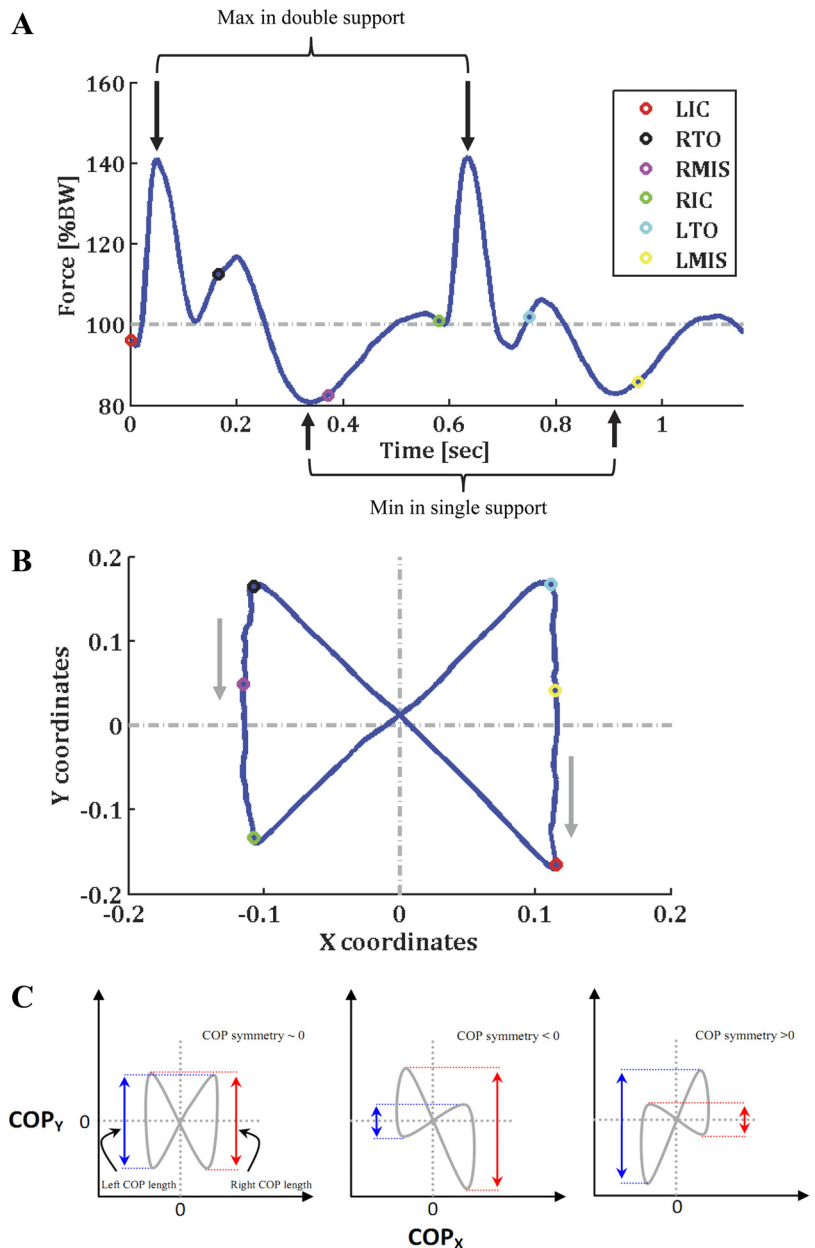

Fig. 2. Representative vertical GRF and center of pressure (COP) profile. *A*: example of vertical GRF for a representative subject during 1 cycle of walking in fast baseline phase. Colored points represent the gait events that were detected: black, red, magenta, green, cyan and yellow points represent left initial contact (LIC), right toe-off (RTO), left midstance (LMIS), right initial contact (RIC), left toe-off (LTO), and right midstance (RMIS), respectively. BW, body weight. *B*: example of COP profile for the same subject during the same cycle. *C*: illustration of the method for calculating COP symmetry. Three examples of COP symmetry values are illustrated: zero (*left*), negative (*center*), and positive (*right*) values. Blue and red double arrows illustrate the left and right COP lengths, respectively.

diately after right toe-off (RTO) or left toe-off (LTO) (Fig. 2*A*). It was previously shown that peaks of the vertical GRF have minimal intraindividual variability and are indicators of weight acceptance and push-up during locomotion (Hesse et al. 1994). Moreover, one of the long-term aims of the present study is to implement such force analysis in gait research study and clinical gait training for individuals suffering from neurological disorder (e.g., individuals with cerebral palsy). Most of the previous studies with neurologically impaired individuals have found that the peaks of GRF were significantly different from those in healthy subjects and it also correlated with the level of motor impairment (Morita et al. 1995; White et al. 1999). For all these reasons, we have chosen the peaks of the GRF as representative force points. Figure 2*A* represents the vertical GRF over time and the gait events for a representative subject during one cycle of walking in the "fast" baseline.

Each gait cycle started at LIC and terminated at the following LIC. Figure 2*B* represents the COP data for the representative subject at the cycle referred to in Fig. 2*A*. The COP profile is clearly characterized by a "butterfly" pattern, which assists in the detection of gait events. As can be seen in Fig. 2*B*, the left single-support phase starts when the right leg is clear of the force plate (RTO) and the left leg remains on the force plate. The COP then progresses backward from the top to the bottom of the butterfly's left wing until the right foot strikes the force plate (RIC). After that, right and left legs are in contact with the force plate and the double-limb support phase starts, the COP progresses diagonally forward to the right wing of the butterfly until the left leg is clear of the force plate (LTO) and the right leg remains on the force plate. The COP then progresses backward from the top to the bottom of the butterfly's right wing until the left foot strikes the force plate (LIC). To summarize, the left and right fore-aft COP segments are essentially the excursion of the foot during left and right single-limb support, respectively, whereas the diagonal COP segments are essentially the excursion of the COP from one side to the other side during double-limb support. COP profiles of each subject were then centered around the origin ($x = 0$, $y = 0$).

The double-support period was defined as the period in time when both feet are in contact with the ground (Ayyappa 1997), namely, the time period between IC of one foot and TO of the other foot. RIC refers to the double-support period when the right foot strikes the ground. LIC refers to the double-support period when the left foot strikes the ground. The single-support period was defined as the period in time when only one foot is in contact with the ground and the second foot is in swing, namely, the period in time between TO of one foot and the subsequent IC of the same foot. Right single support refers to the single-support period when the right foot is in contact with the ground and the left foot is in the swing phase. Similarly, left single support refers to the single-support period when the left foot is in contact with the ground and the right foot is in the swing phase.

Motor adaptation occurs when the brain, in response to the current prediction error, changes the motor commands of the internal model in the subsequent trial (Thoroughman and Shadmehr 2000). In the present study, we defined the peaks of GRF as the controlled output of the motor system. Since the peaks of GRF changed with walking speed, motor adaptation of the GRF refers to a short-timescale motor learning process that occurs when the brain changes the motor commands according to the current motor error resulting from speed perturbation. Motor error was defined as the discrepancy between expected and actual dynamics of the system. Hence, we measured the "GRF change" as the motor error variable that drives the motor system for adaptation. In each gait cycle, if the expected walking speed is identical to the actual speed, no motor error occurs and the "force change" decreases to zero. The GRF change of each leg in each cycle was calculated as the difference between GRF peak and the average of the GRF peak of the same leg at the same speed in the baseline phase. For example, to quantify the GRF change of the right leg (fast leg) at IC during the adaptation phase, we calculate the difference between the GRF peak after RIC during adaptation and the

average of the GRF peak after RIC during fast baseline. Similarly, to quantify the GRF change of the left leg (slow leg) at IC during the adaptation phase, we calculate the difference between the GRF peak after LIC during adaptation and the average of the GRF peak after LIC during the slow baseline. We calculate the adaptation measure for each leg during single- and double-support periods. During adaptation, a zero value of the GRF change indicates full adaptation while a nonzero value indicates an unadapted pattern.

We also measured the difference of GRF between legs as an interlimb "force symmetry" measure (Kim and Eng 2003). The GRF difference in each cycle was calculated as the difference between the GRF peak of the left leg (slow leg) and the GRF peak of the right leg (fast leg). A zero value of the "GRF difference" indicates force symmetry between legs, while a nonzero value indicates force asymmetry.

To examine adaptation of the COP we introduced a third measure, the COP symmetry, as follows:

$$\text{COP symmentry} = \frac{\text{left COP length} - \text{right COP length}}{\text{left COP length} + \text{right COP length}} \quad (1)$$

where left COP length was calculated as the *y*-distance in the COP profile between consecutive LTO and RIC and right COP length was calculated as the *y* (anterior-posterior)-distance between consecutive RTO and LIC (Fig. 2*C*). The difference in each cycle was then normalized to the sum of the right and left COP lengths.

During adaptation, force change, force symmetry, and COP symmetry parameters represent the amount of motor errors in a given cycle. When these parameters are equal to 0 during the adaptation phase, subjects had fully adapted to the external perturbations and few motor errors occurred, while positive or negative values of these parameters indicate that the subject failed to adapt.

A dual-rate exponential function (Smith et al. 2006) was fitted to COP symmetry and to force symmetry data points during split-belt adaptation to characterize the adaptation processes that drive the limb kinetic. This model had four free parameters: two gains, A_1 and A_2, and fast and slow time constants, B_{fast} and B_{slow}, respectively:

$$E(n) = A_1 \cdot e^{(-B_{\text{fast}} \cdot n)} + A_2 \cdot e^{(-B_{\text{slow}} \cdot n)} \quad (2)$$

Where $E(n)$ was the computed limb error on cycle *n*. COP symmetry and force data were normalized to each max error before curve fitting. The free parameters of this model were fitted with MATLAB software with Curve Fitting Toolbox (The MathWorks, Natick, MA).

Statistical analysis. Statistical analysis of the data was performed with MATLAB software with Statistics Toolbox (The MathWorks). To compare the different parts of the experiment, we first calculated the average across subjects of the last five cycles (Choi et al. 2009; Reisman et al. 2005) in each baseline phase (first slow baseline, fast baseline, and second slow baseline, respectively), the average of the first and last five cycles in the adaptation phase (early and late adaptation, respectively), and the average of the first and last five cycles in the postadaptation phase (early and late postadaptation, respectively; Reisman et al. 2005). We defined baseline slow 1, baseline fast, baseline slow 2, early adaptation, late adaptation, early postadaptation, and late postadaptation blocks as the average of the last five cycles of the first slow baseline, the last five cycles of the fast baseline, the last five cycles of the second slow baseline, the first five cycles of the adaptation phase, the last five cycles of the adaptation phase, the first five cycles of the postadaptation phase, and the last five cycles of the postadaptation phase, respectively. Repeated-measures ANOVA was used to compare testing periods for kinetic parameters. When the ANOVA revealed significant differences, the Bonferroni post hoc test was used to compare testing periods. Significance level was set to 0.05.

RESULTS

We asked subjects to walk on a custom split-belt force treadmill while we implicitly changed the speed of the belts. During the baseline and postadaptation phases the belts moved together at similar speeds, while in the adaptation phase the belts moved separately at different speeds. All subjects completed the walking phases without any declared fatigue.

Feedforward adaptation of forces at initial contact. For all subjects, we found that the maximum GRF at IC for both legs changed gradually during the split-belt adaptation phase and showed significant aftereffects. Figure 3 illustrates the change of the GRF of the right and left legs during the first 600 cycles in adaptation (Fig. 3, *A* and *B*, respectively) and the first 150 cycles during postadaptation (Fig. 3, *C* and *D*, respectively). GRF profiles are marked with a color gradient, indicating initial cycle to late cycle. Each trace in Fig. 3 represents the average GRF across all subjects. In all cases, peaks of the GRF at IC are shown as colored points at $t = 0.4$ s (Fig. 3). In early adaptation, the GRF of the right leg at IC started with low values compared with the baseline phase. However, with time these forces increased slowly to achieve a plateau (Fig. 3A). In contrast, the GRF of the left leg at IC started with high values and with practice the forces diminished to a steady-state value (Fig. 3B). Interestingly, we showed the reverse pattern during postadaptation for both legs (Fig. 3, *C* and *D*, for right and left legs, respectively). To quantify the motor adaptation of each leg and establish whether an "aftereffect" had occurred, we measured the change of the GRF produced in each cycle. The GRF change

of each leg in each cycle was calculated as the difference between the GRF and the average of the GRF of the same leg at the same speed in the baseline phase. Figure 4*A* shows the average GRF change across subjects of the right leg during baseline, adaptation, and postadaptation. During early adaptation, there was a negative value of GRF change such that the right leg produced lower forces than it produced previously in the fast baseline. This negative value of GRF change increased slowly throughout the adaptation phase. Importantly, in early postadaptation phase, there was a clear motor aftereffect such that the right leg produced higher forces than it produced in the second slow baseline. This reverse pattern gradually returned to slow baseline values. Figure 4*B* shows the average GRF change of the left leg during the different phases of the experiment. We found a similar pattern of adaptation and aftereffect in the left leg forces. However, during early adaptation, there was a positive value of GRF change such that the left leg produced higher forces than it produced previously in the second slow baseline. This positive value decreased slowly through the adaptation phase. In early postadaptation, the left leg also showed an aftereffect, such that the left leg produced lower forces than it produced in the second slow baseline. In late postadaptation, the GRF change gradually achieved a pattern similar to baseline. Figure 4, *C* and *D*, show the "force change" at IC averaged over the five cycles taken from each phase (for right and left legs, respectively). In both legs, a repeated-measures ANOVA showed a significant effect of force change during the different experiment phases [$F(6,49) = 76.93$, $P <$
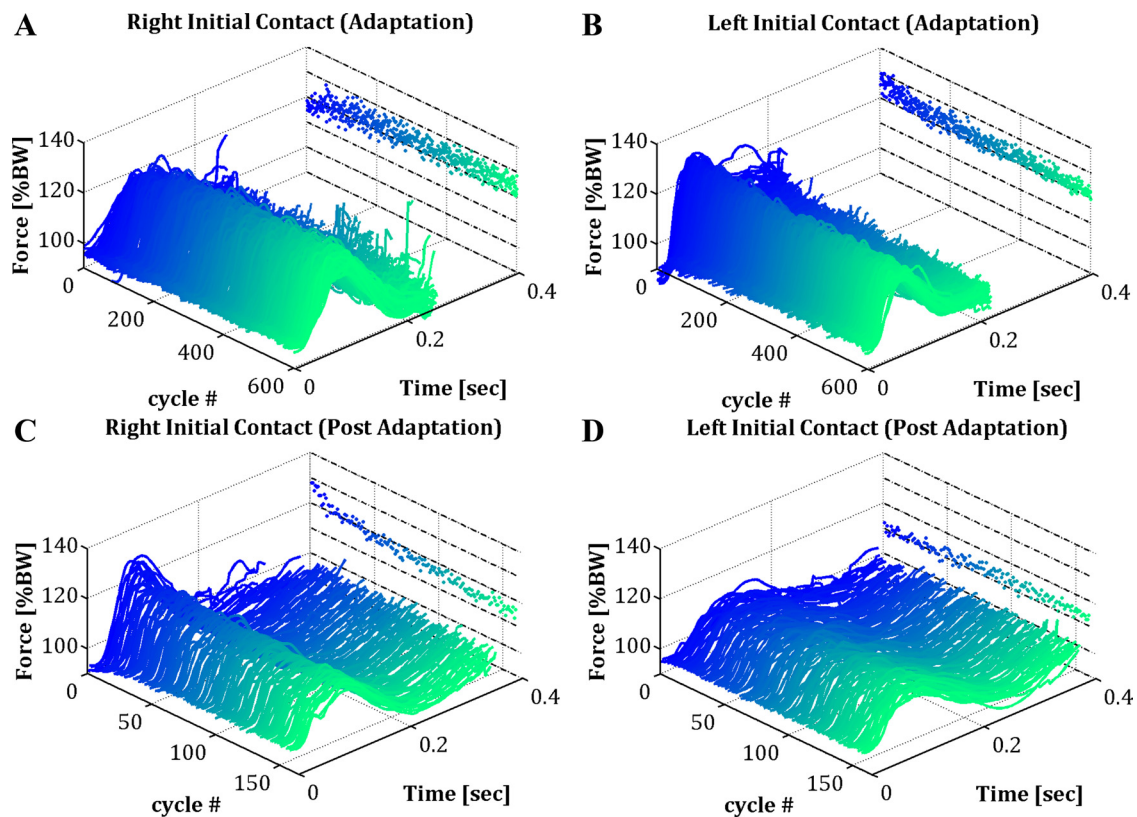

Fig. 3. GRF during adaptation and postadaptation. Each profile represents the average GRF across all subjects. GRF profiles are marked with a color gradient ranging from blue to green, indicating initial cycle to late cycle, respectively. *A*: average GRF of the RIC during the first 600 cycles in adaptation. *B*: average GRF across subjects of the LIC during the first 600 cycles in adaptation. *C*: average GRF across subjects of the RIC during the first 150 cycles in postadaptation. *D*: average GRF across subjects of the LIC during the first 150 cycles in postadaptation. In all cases, the peaks of the GRF at ICs are shown as colored points at $t = 0.4$ s.
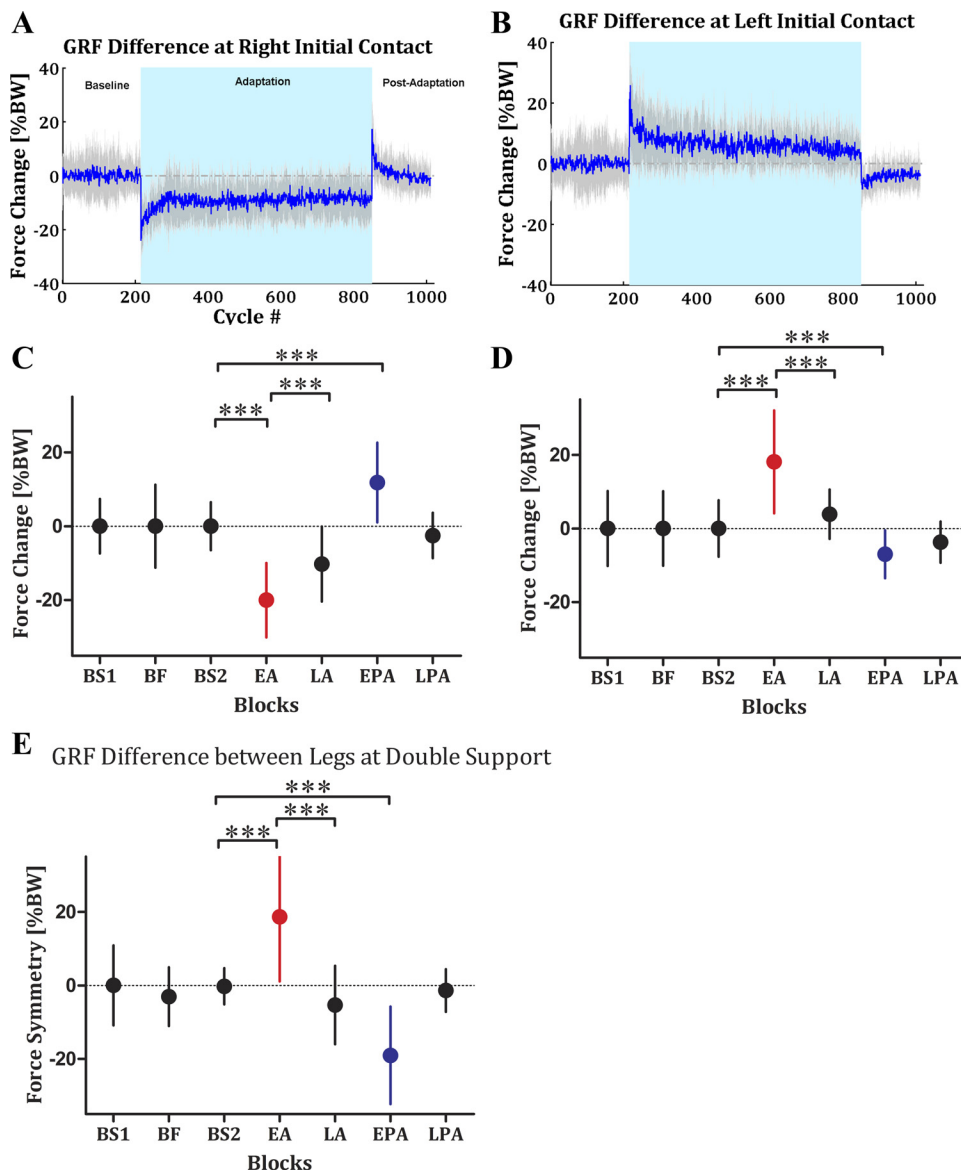
Fig. 4. Feedforward adaptation of the GRF at IC. *A*: GRF change of the RIC across testing periods (3 baselines, adaptation, and postadaptation). Solid blue line is mean GRF change across subjects, and shaded area is SDs. *B*: GRF change of the LIC across testing periods (3 baselines, adaptation, and postadaptation). Similarly, solid blue line is mean GRF change across subjects and shaded area is SDs. *C* and *D*: group data analysis of the average "GRF change" of RIC (*C*) and LIC (*D*). Each data point represents the average over 5 cycles from the early or late portions of each testing phase for each subject individually and then averaged across all subjects in the group. BS1, BF, BS2, EA, LA, EPA, and LPA blocks represent the average of the last 5 cycles in the 1st slow baseline phase, last 5 cycles in the fast baseline phase, last 5 cycles in the 2nd slow baseline phase, first 5 cycles in the adaptation phase, last 5 cycles in the adaptation phase, first 5 cycles in the postadaptation phase, and last 5 cycles in the postadaptation phase, respectively. Red data points represent average value of the force change in early adaptation, and blue data points represent average value of the force change in early postadaptation. Error bars indicate SDs. *E*: group data of the force symmetry at IC between left and right leg averaged over the 5 cycles taken from each phase. ***Significance level of $P < 0.0001$.

0.0001 and $F_{(6,49)} = 48.04$, $P < 0.0001$ for right and left legs, respectively]. Bonferroni's post hoc analysis indicated that subjects changed the GRF from both slow baseline phases to early adaptation ($P < 0.0001$), adapted to speed perturbation and reduced the absolute GRF change from the early adaptation to late adaptation phase ($P < 0.0001$), and showed a significant motor aftereffect in early postadaptation ($P < 0.001$). Figure 4*E* shows group data for the force symmetry at IC between left and right legs. There was a significant main effect of force symmetry during the different phases [$F_{(6,49)} = 51.98$, $P < 0.0001$]. Bonferroni's post hoc analysis indicated that subjects changed the GRF between legs at double support from both of the slow baseline phases to the early adaptation ($P < 0.0001$), adapted to speed perturbation and showed significant change from early adaptation to late adaptation phase ($P < 0.0001$), and showed significant aftereffect (baseline vs. early postadaptation phases; $P < 0.0001$). These observations of gradual adaptation and aftereffects of learning clearly indicate the generation of internal models in a feedforward control scheme.

Feedback control of forces at single support. For all subjects, we found that the minimum GRF at single support—defined as the time period when only one foot is in contact with the ground and the second foot is in swing—for both legs changed immediately in early adaptation and showed little change during adaptation. In early postadaptation phase, there was no significant aftereffect (Fig. 5, *A* and *B*). Figure 5*C* shows group data for the difference of the GRF at single support between left and right legs. There was a significant main effect of force change during the different phases [$F_{(6,39)} = 10.99$, $P < 0.0001$]. Bonferroni's post hoc analysis indicated that subjects changed the GRF between legs at single support from both slow baseline phases to early adaptation ($P < 0.0001$). However, the GRF between legs did not adapt to speed perturbation and showed very little change from early adaptation to late adaptation phase ($P > 0.9$) and from baseline phase to early postadaptation phase ($P > 0.25$). During single-limb support, both the immediate change of the GRF in early adaptation and the absence of the motor aftereffect in early postadaptation support feedback control mechanism.
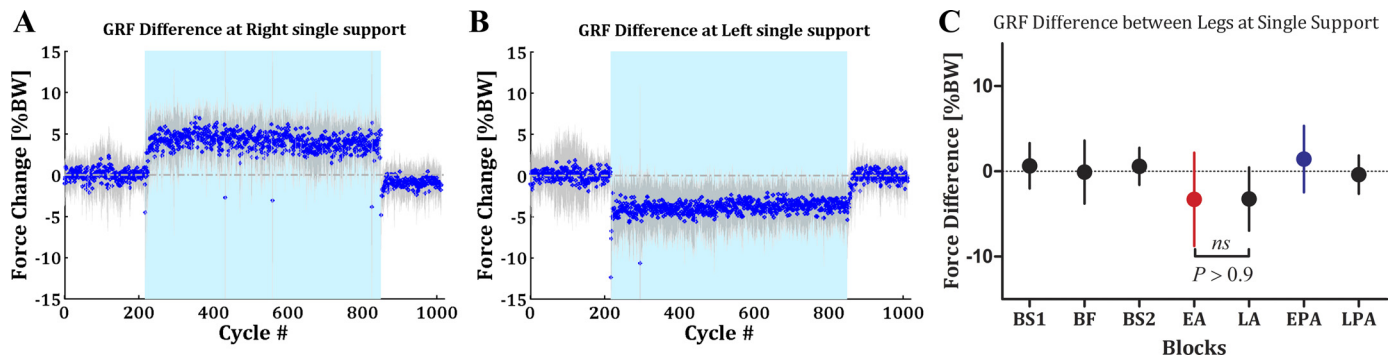
Fig. 5. Feedback adaptation of the GRF at single support. *A*: right leg GRF change at single support across testing periods (3 baselines, adaptation and postadaptation). Solid blue line is the average GRF change across subjects, and shaded area is SDs. *B*: left leg GRF change at single support across testing periods (3 baselines, adaptation and postadaptation). Similarly, solid blue line is the average GRF change across subjects and shaded area is SDs. *C*: group data of the force difference at single support between left and right legs. Each data point represents the average over 5 cycles from the early or late portions of each testing phase for each subject individually and then averaged across all subjects in the group. Error bars indicate SDs. ns, Not statistically significant.

Feedforward adaptation of COP. Figure 6A shows the COP profiles of the first 50 cycles for a representative subject. During the two slow and fast baseline phases, the COP butterfly patterns were symmetric around the origin point (0, 0) with similar wing length on the right and left sides of the COP. Right and left wing lengths of the COP butterfly were greater in fast baseline than in the two slow baselines. However, during the adaptation phase the COP butterfly patterns became asymmetric: the right wing was longer than the left wing. During postadaptation, we observed a clear aftereffect in the COP profile. The COP butterfly patterns reversed the asymmetry around the origin point (0, 0) compared with the COP profiles during the adaptation phase. COP profiles of the first 50 cycles are marked with a color gradient ranging from light blue to dark blue in Fig. 6A, indicating initial cycle to late cycle, respectively. During early adaptation, the distance between RIC and LTO is less than the distance between LIC and RTO. Figure 6B shows the average "COP symmetry" across subjects during baseline, adaptation, and postadaptation phases. During the baseline phases, COP symmetry values were close to zero, indicating a symmetric pattern of locomotion. However, during early adaptation, there was a negative value of COP symmetry indicating that the left COP length was less than the right COP length. This negative value of the COP symmetry increased slowly throughout the adaptation phase. In the early postadaptation phase, there was a clear positive motor aftereffect of the COP pattern: the left COP length was greater than the right COP length. This reverse pattern gradually
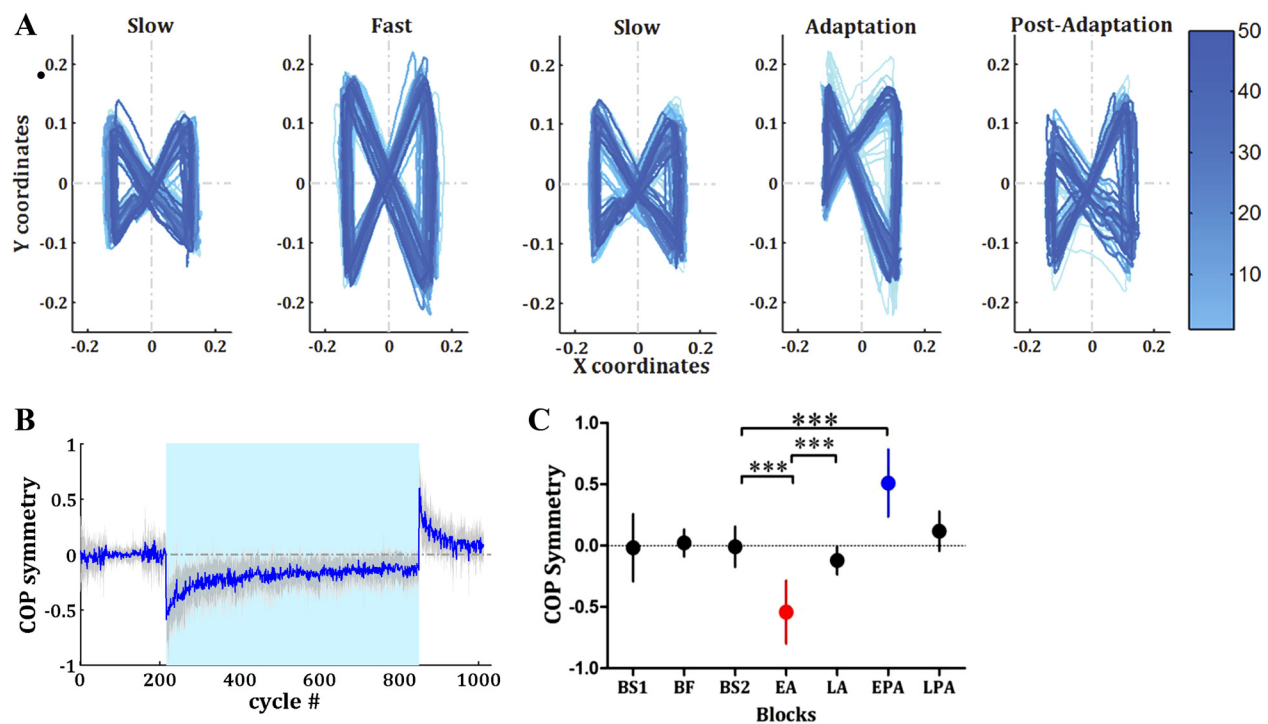

Fig. 6. Feedforward adaptation of the COP. *A*: COP profiles of the first 50 cycles for a representative subject during 2 slow baselines, fast baseline, adaptation, and postadaptation periods. COP profiles are marked with a color gradient ranging from light blue to dark blue, indicating initial cycle to late cycles, respectively. *B*: COP symmetry measurement across testing periods. Solid blue line is the average COP symmetry across subjects, and dashed area is SDs. *C*: group data analysis of the COP. Each data point represents the average over 5 cycles from the early or late portions of each testing phase for each subject individually and then averaged across all subjects in the group. Error bars indicate SDs. ***Significance level of $P < 0.0001$.

returned to zero value as baseline values. Figure 6C shows group data for the COP slope. There was a significant main effect during the different phases [$F(6,49) = 115.4$, $P < 0.0001$]. Bonferroni's post hoc analysis indicated that COP symmetry changed between the two slow baseline phases to the early adaptation phase ($P < 0.0001$). The COP symmetry adapted to speed perturbation and showed significant change from early adaptation to late adaptation phase ($P < 0.0001$) and showed significant motor aftereffect (2 baselines vs. early postadaptation phase; $P < 0.0001$).

Two timescales in locomotor adaptation. We fitted the dual-rate exponential function (adaptation curve) with fast and slow time constants to COP and force symmetry (data not shown) data points during adaptation. Figure 7A shows the net adaptation curve fit to the average COP symmetry across subjects, the fast process, and the slow process. Accuracy of fit was quantified by measuring the coefficient of determination R^2. We found that both curves fitted the data well ($R^2 = 0.81$ and 0.63 for COP and force symmetry, respectively). The estimated parameters (with 95% confidence intervals) are $A_1 = -0.4955$ (-0.5379, -0.4531), $A_2 = -0.427$ (-0.4517, -0.4023), $B_{fast} = 0.02527$ (0.02095, 0.0296), and $B_{slow} = 0.001115$ (0.0009627, 0.001267) for the average COP symmetry and $A_1 = -0.4503$ (-0.5034, -0.3971), $A_2 = -0.3913$ (-0.4051, -0.3775), $B_{fast} = 0.04863$ (0.03926, 0.058), and $B_{slow} = 0.0005726$ (0.0004761, 0.0006691) for the force symmetry. Group results from analysis of the fast and slow time constants revealed that the two rates of the COP symmetry adaptation curve are similar to the adaptation rates of the force symmetry (Fig. 7B). Difference between COP and force symmetry did not reach statistical significance for the fast process [2-tailed t-test, $t(18) = 0.73$, $P = 0.48$] or for the slow process [2-tailed t-test, $t(18) = 1.1$, $P = 0.29$]. Note that the comparison of the time course was between COP symmetry (Fig. 6B) and force symmetry (difference between Fig. 4A and Fig. 4B).

DISCUSSION

We report here three main findings. First, both the GRF at IC parameter and the COP parameter were stored, changed slowly during adaptation, and presented a robust aftereffect during postadaptation, suggesting feedforward adaptive control of these parameters. Second, GRF at single support reacted immediately to speed perturbation during split-belt adaptation and did not show any aftereffect in postadaptation, suggesting feedback rather than adaptive control of this parameter. Third, the locomotor adaptation is characterized by two timescales.

Kinetics vs. kinematics adaptation. Previous studies have shown that the central nervous system (CNS) stores a new pattern of the interlimb spatial and temporal locomotor parameters (Reisman et al. 2005). They used a split-belt treadmill to perturb the locomotor pattern and found that step length and double-support time as interlimb measures were controlled by a feedforward predictive controller and verified this by observing the presence of aftereffects when the perturbation was removed. However, the stride length and the single-support time as intralimb measures adapted immediately, and they suggested that these parameters were controlled by a feedback reactive controller. Our kinetic results are consistent with kinematic results shown previously by Reisman et al. (2005). We found here that the peak of GRF of each leg in the single-support period reacts quickly to speed perturbations and is controlled by feedback mechanism. Markedly, we found that the peak of GRF of each leg at foot contact was stored and controlled by predictive feedforward control. We show here that there is a difference between the force adaptation at single- and double-support periods during adaptation to a split-belt force treadmill. These results suggest independent adaptation processes of single-support and double-support forces.

During the swing phase, walking speed cannot be estimated under pure feedback control because of the absence of leg contact, since biological feedback loops need sensory information from the environment. In this phase, a feedforward control scheme, as suggested in studies related to reaching movements (Kawato 1999; Wolpert et al. 1998), must be dominant. In such feedforward control, during motor adaptation the CNS acquires an inverse dynamics model of the external perturbation to minimize the expected motor error. Since the IC is defined as a fast event (approximately the first 100 ms) in the double-limb support phase and is linked to the second phase of swing (Halbertsma 1983), the GRF cannot be executed under feedback control and the CNS must predict the GRF via composition of an internal model of the imposed walking speed by using adaptive feedforward control. One way to verify the created internal model is the presence of motor aftereffect, when the internal model does not fit the external perturbation or lack of perturbation (Shadmehr and Mussa-Ivaldi 1994). In our experiment aftereffects are observed when the speed perturbation is unexpectedly removed (Fig. 4 and Fig. 6). Conversely, the motor system received direct sensory information about the speed of walking with sensory feedback mechanism in the stance phase (single-limb support), and in this phase no aftereffects were observed.
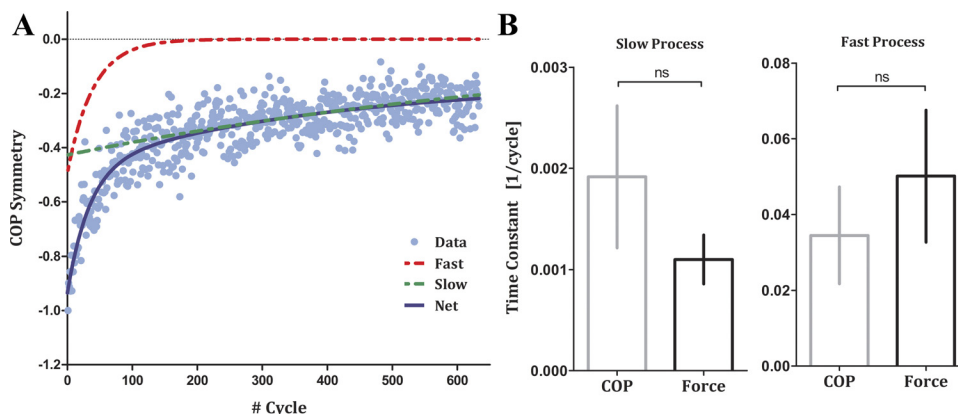

Fig. 7. Dual-rate adaptation curve. *A*: normalized COP symmetry during the adaptation phase and the model fit. Light blue data points are mean COP symmetry across subjects from the adaptation phase, and the dark blue curve is the fit for the dual-rate model. Dashed red and green lines are the fast and slow exponent functions, respectively. *B*, *left*: the model's slow time constant averaged across subjects. *Right*: the model's fast time constant averaged across subjects. Gray and black bars represent COP and force data points, respectively. Error bars indicate SEs.

It is important to note that we defined the change of the GRF as the motor error that drives motor adaptation during locomotion. Another study has also suggested that kinetic error (e.g., joint moments) drives the locomotor adaptation during walking with a robotic exoskeleton device (Kao et al. 2010). However, it is possible to think of the motor adaptation process driven by kinematic motor error. For example, Reisman et al. (2005) proposed that sensory kinematic error (e.g., step symmetry) drives locomotor adaptation during walking on a split-belt treadmill. The present study cannot dissociate a causal relationship between kinetic (e.g., force) and kinematic (e.g., position) control as well as distinguish between possible distinct adaptation processes. Therefore, our force-dependent adaptation process can be modeled and replaced effectively by a position-dependent adaptation process. Further studies are needed to provide more insight into the nature of the error-dependent process driving motor adaptation in locomotion.

Locomotor adaptation and central pattern generators. Our findings are consistent with the suggestion that locomotion is based on central pattern generators (CPGs), defined as neural networks capable of producing coordinated patterns of rhythmic activity (Grillner et al. 1998). During normal locomotion, the cycle period varies as a function of the stance phase while the swing phase remains relatively invariant, a basic feature of the spinal CPG (Goslow et al. 2005; Grillner et al. 1979, 1998). Swing has a fixed duration, regardless of speed of locomotion, because it is controlled only by a motor program, while the stance phase is of variable duration depending on speed and is regulated by sensory feedback. IC is defined as the very short event when the foot touches the ground and is linked to the second phase of swing in which the knee and ankle start to extend in preparation for IC. One of the most important events in walking is the foot touchdown, i.e., the end of the swing extension phase (Halbertsma 1983). The proper control of this event is important for ensuring proper foot positioning for accepting weight and providing a stable support at IC. This short phase appears to be controlled by a motor program that aims to preset a mechanical condition of the lower extremity leading to the maintenance of an extended configuration of the main body segments in preparation for impact with the ground (Crenna et al. 2001). Our results demonstrate robust aftereffect during postadaptation at IC and strengthen the affiliation of the IC to the swing phase as part of a motor program, while the absence of aftereffects at single support endorses the general agreement that the interaction of the foot with the environment is regulated by sensory inputs.

Balance, stability, and COP. COP has been used as an index to calculate the balance of individuals. It reflects balance and the effect of different treatment modalities on the lower limb (Sakaguchi et al. 1994). Several studies have used COP analysis to demonstrate increased postural sway during quiet standing and its association with elevated fall risk in older adults (Maki et al. 1994; Melzer et al. 2001). Other studies showed the influence of different training programs in improving balance and reducing the COP sway area in chronic stroke patients and the elderly (Hass et al. 2004; Tsaklis et al. 2012). Adaptation of the COP during locomotion might be critical for body stability. In the present study, modification of COP profiles was clearly shown in early adaptation. In this phase, the distance between RIC and LTO is shorter than the distance between LIC and RTO (Fig. 6). The conventional claim has been that COP

symmetry improves stability and that COP asymmetry is a marker of pathology and reduced balance (Nichols 1997; Woollacott and Shumway-Cook 2005). This claim was based on force plates that measure postural sway (stability in standing) and symmetry in standing: symmetry measures reflect the amount of weight on each foot or the distance of the COP away from the midline. In previous research, COP has been used as a good index to calculate the balance of individuals in standing (Karlsson and Frykberg 2000; Önell 2000). Additionally, walking is a dynamic rhythmic activity, in which the step-by-step stability may be quite different from posture. This may therefore dictate differences in active control as well as how sensory information is integrated and used for step-by-step stabilization. Walking rhythmically places the body center of mass beyond the base of support, interpreted previously as "controlled falling" (Perry and Davids 1992). Furthermore, the development of treadmills with embedded force plates opens the way to direct analysis of GRF and COP during walking. Understanding COP dynamics in normal gait is intuitively helpful in understanding several capabilities such as muscular coordination, balance, strength and joint kinematics (Winter 1991). A recent study has examined the role of vision in the control of balance during walking, using COP variability as an indicator of the degree of integrative control during both walking and standing (O'Connor and Kuo 2009). An understanding of how the COP motion is generated and controlled continuously during locomotion may contribute to an understanding of pathologies. For example, Jamshidi et al. (2010) concluded in their studies that the excessive difference in anterior-posterior COP trajectory between a normal and a drop foot subject during gait may lead to a loss of balance. Taken together these results suggest that COP measurement during walking and standing is essential for understanding gait stability and might be used for further understanding of walking performance in persons suffering from neurological disorders. Therefore, it is possible that stability criteria may lead to optimizing force symmetry and COP symmetry measurements during locomotor adaptation.

Dual rate in locomotor adaptation. Recent studies in hand motor control have suggested that the adaptation process can be modeled by a dual-rate adaptive model (Lee and Schweighofer 2009; Smith et al. 2006). This model was suggested to explain the trial-by-trial adaptation of motor errors. This dual-rate model suggests that the net adaptation is a result of summing slow and fast exponential adaptation processes. In our study, we used this two-rate exponential function to model the kinetic errors (COP and force symmetry). Here we show that the dual-state adaptation process can properly account for the motor errors in adaptation to a split-belt treadmill (Fig. 7A). We found that the force adaptation and COP adaptation curves behaved similarly and had similar time constants (Fig. 7B). The suggested multiple-timescale adaptive process during split-belt locomotor adaptation might explain the nature of motor memory in learning and forgetting such novel motor tasks. It was suggested that learning new motor tasks involves a fast process that reacts rapidly to motor error but has weak memory retention, together with a slow process that reacts slowly to motor error but significantly exhibits strong retention (Shadmehr and Mussa-Ivaldi 2012; Smith et al. 2006). Although the present study did not examine memory saving in a readaptation after deadaptation paradigm, the suggested dual-state model is

sufficiently able to account for the trial-by-trial errors that drive the adaptive response to a split-belt treadmill observed in our study. Memory retention and saving during locomotor adaptation have been recently studied with the split-belt treadmill system (Malone et al. 2011). In this study, Malone et al. (2011) found that different adaptation structures significantly affect the retention of the motor memory during readaptation on the subsequent day. They observed faster relearning (i.e., memory saving) on the second day when subjects adapted and deadapted several times on the first day. The suggested dual-rate adaptive model properly explains these results. The basic idea of the dual-rate model is that removal (e.g., absence of external perturbation during the time period between the 2 days) or reversal (e.g., opposing perturbation during the first day) of the perturbation may return motor behavior to baseline, but not by completely erasing memories of what it has learned. Although it appears that the dual-rate model successfully accounts for locomotion data, further behavioral and neuroimaging studies are needed to better investigate the suitability of the dual-rate model for accounting for memory saving while relearning novel locomotor tasks. Understanding the adaptive processes during different locomotor adaptation will give us fundamental insights into understanding motor memory formation during locomotion. Moreover, our findings are consistent with previous studies and support the multiple-timescale model that drives motor adaptation while learning novel motor tasks (Hatada et al. 2006; Kojima et al. 2004; Smith et al. 2006). Furthermore, this dual-rate adaptation process is consistent with previous cerebellum studies that support the findings of motor learning and provide evidence of the neural basis of the fast and slow processes (Medina et al. 2001; Ohyama and Mauk 2001).

Neural basis of locomotor adaptation. Several studies have suggested that the cerebellum plays a key role in feedforward adaptation to a novel environment, and it was suggested that the cerebellum used sensory prediction errors to change a forward model (Kawato et al. 2003; Morton and Bastian 2006; Tseng et al. 2007; Wolpert et al. 1998). Studies in cerebellar damage confirmed this interpretation. Smith and Shadmehr (2005) asked patients with cerebellar damage to make reaching movements while a manipulandum robot applied velocity-dependent force perturbations to their hands. They found that cerebellar patients are impaired in their predictive adaptation. Similar adaptation studies have been done for lower limb movements. Recent studies of neural control of locomotion using a split-belt treadmill suggest that damage in the cerebellum area would significantly affect the adaptation of the limb coordination (Morton and Bastian 2006). The finding of this study was supported by previous neurophysiological work conducted in cats in which the locomotor adaptation was interfered with by intentional damage of the cat's cerebellum (Yanagihara and Kondo 1996). Furthermore, the involvement of the cerebellum in locomotor adaptation has been shown in various experiments conducted predominantly in cerebellar patients (Ilg et al. 2007, 2008; Morton and Bastian 2004, 2006). Additionally, a recent study using the split-belt treadmill tool has indicated that independent functional networks control the two directions of walking (i.e., forward and backward walking). They postulated that the cerebellum is involved in such distinct neural networks (Choi et al. 2009). Many other works have suggested that the cerebellum is the anatomical site

for the formation of internal models as well as the site involved in predictive motor memory storage (Atkeson 1989; Diedrichsen et al. 2005; Kawato et al. 1987; Tseng et al. 2007). To conclude, all these works make the cerebellum the strong candidate responsible for motor adaptation during locomotion in general and during split-belt locomotion in particular. However, involvement of cortical and subcortical areas as well as interactions between the cerebellum and these areas should not be entirely ignored (Stubbs and Gervasio 2012). Therefore, the contribution of the cerebellum and the cerebral cortex to the adaptive change of the GRF during locomotor adaptation is still unclear, and the exact role of the cerebellum and cerebral cortex in GRF adaptation might be better understood by testing adaptation to a split-belt force treadmill with patients suffering from cerebellar and cerebral damage or by applying TMS over different brain areas.

In conclusion, the main results of the present study reveal that during adaptation to the split-belt force treadmill subjects altered the interlimb GRF slowly, using feedforward predictive control and showing robust aftereffects during early postadaptation. However, subjects altered the intralimb GRF rapidly, using feedback control, and showed no aftereffect. The COP profile gradually changed during adaptation and showed significant aftereffect during early postadaptation. Finally, the locomotor adaptation process can be modeled by a dual-rate adaptive model. Future studies of GRF and COP during adaptation to the split-belt force treadmill are required to better understand the neural control of locomotion and to provide new rehabilitation procedures such as reducing the chance of fall in the elderly population and enhancing adaptation in cerebellar and cerebral patients.

DISCLOSURES

No conflicts of interest, financial or otherwise, are declared by the author(s).

AUTHOR CONTRIBUTIONS

Author contributions: F.M., T.H., S.B.-H., and A.K. conception and design of research; F.M. and T.H. performed experiments; F.M. and T.H. analyzed data; F.M., T.H., S.B.-H., and A.K. interpreted results of experiments; F.M. and T.H. prepared figures; F.M. drafted manuscript; F.M., T.H., S.B.-H., and A.K. edited and revised manuscript; F.M., T.H., S.B.-H., and A.K. approved final version of manuscript.

REFERENCES

Atkeson CG. Learning arm kinematics and dynamics. *Annu Rev Neurosci* 12: 157–183, 1989.

Ayyappa E. Normal human locomotion, part 1: basic concepts and terminology. *J Prosthetics Orthotics* 9: 10–17, 1997.

Blanchette A, Moffet H, Roy JS, Bouyer LJ. Effects of repeated walking in a perturbing environment: a 4-day locomotor learning study. *J Neurophysiol* 108: 275–284, 2012.

Cavanagh PR, Lafortune MA. Ground reaction forces in distance running. *J Biomech* 13: 397–406, 1980.

Chib VS, Krutky MA, Lynch KM, Mussa-Ivaldi FA. The separate neural control of hand movements and contact forces. *J Neurosci* 29: 3939–3947, 2009.

Choi JT, Vining EP, Reisman DS, Bastian AJ. Walking flexibility after hemispherectomy: split-belt treadmill adaptation and feedback control. *Brain* 132: 722–733, 2009.

Crenna P, Cuong DM, Brénière Y. Motor programmes for the termination of gait in humans: organisation and velocity-dependent adaptation. *J Physiol* 537: 1059–1072, 2001.

Cunningham DA, Rechnitzer PA, Pearce ME, Donner AP. Determinants of self-selected walking pace across ages 19 to 66. *J Gerontol* 37: 560–564, 1982.

Diedrichsen J, Verstynen T, Lehman SL, Ivry RB. Cerebellar involvement in anticipating the consequences of self-produced actions during bimanual movements. *J Neurophysiol* 93: 801–812, 2005.

Donchin O, Francis JT, Shadmehr R. Quantifying generalization from trial-by-trial behavior of adaptive systems that learn with basis functions: theory and experiments in human motor control. *J Neurosci* 23: 9032–9045, 2003.

Emken JL, Reinkensmeyer DJ. Robot-enhanced motor learning: accelerating internal model formation during locomotion by transient dynamic amplification. *IEEE Trans Neural Syst Rehabil Eng* 13: 33–39, 2005.

Flanagan JR, Rao AK. Trajectory adaptation to a nonlinear visuomotor transformation: evidence of motion planning in visually perceived space. *J Neurophysiol* 74: 2174–2178, 1995.

Flanagan JR, Wing AM. The role of internal models in motion planning and control: evidence from grip force adjustments during movements of hand-held loads. *J Neurosci* 17: 1519–1528, 1997.

Fortin K, Blanchette A, McFadyen BJ, Bouyer LJ. Effects of walking in a force field for varying durations on aftereffects and on next day performance. *Exp Brain Res* 199: 145–155, 2009.

Gordon KE, Ferris DP. Learning to walk with a robotic ankle exoskeleton. *J Biomech* 40: 2636–2644, 2007.

Goslow GE, Reinking RM, Stuart DG. The cat step cycle: hind limb joint angles and muscle lengths during unrestrained locomotion. *J Morphol* 141: 1–41, 2005.

Grillner S, Ekeberg Ö, El Manira A, Lansner A, Parker D, Tegnér J, Wallén P. Intrinsic function of a neuronal network—a vertebrate central pattern generator. *Brain Res Rev* 26: 184–197, 1998.

Grillner S, Halbertsma J, Nilsson J, Thorstensson A. The adaptation to speed in human locomotion. *Brain Res* 165: 177–182, 1979.

Halbertsma JM. The stride cycle of the cat: the modelling of locomotion by computerized analysis of automatic recordings. *Acta Physiol Scand Suppl* 521: 1–75, 1983.

Hass CJ, Gregor RJ, Waddell DE, Oliver A, Smith DW, Fleming RP, Wolf SL. The influence of Tai Chi training on the center of pressure trajectory during gait initiation in older adults. *Arch Phys Med Rehabil* 85: 1593–1598, 2004.

Hatada Y, Miall RC, Rossetti Y. Long lasting aftereffect of a single prism adaptation: directionally biased shift in proprioception and late onset shift of internal egocentric reference frame. *Exp Brain Res* 174: 189–198, 2006.

Hesse SA, Jahnke MT, Bertelt CM, Schreiner C, Lücke D, Mauritz KH. Gait outcome in ambulatory hemiparetic patients after a 4-week comprehensive rehabilitation program and prognostic factors. *Stroke* 25: 1999–2004, 1994.

Ilg W, Giese M, Gizewski E, Schoch B, Timmann D. The influence of focal cerebellar lesions on the control and adaptation of gait. *Brain* 131: 2913–2927, 2008.

Ilg W, Golla H, Thier P, Giese MA. Specific influences of cerebellar dysfunctions on gait. *Brain* 130: 786–798, 2007.

Jamshidi N, Rostami M, Najarian S, Menhaj MB, Saadatnia M, Salami F. Differences in center of pressure trajectory between normal and steppage gait. *J Res Med Sci* 15: 33–40, 2010.

Kao PC, Ferris DP. Motor adaptation during dorsiflexion-assisted walking with a powered orthosis. *Gait Posture* 29: 230–236, 2009.

Kao PC, Lewis CL, Ferris DP. Short-term locomotor adaptation to a robotic ankle exoskeleton does not alter soleus Hoffmann reflex amplitude. *J Neuroeng Rehabil* 7: 33, 2010.

Karlsson A, Frykberg G. Correlations between force plate measures for assessment of balance. *Clin Biomech* 15: 365–369, 2000.

Kawato M. Internal models for motor control and trajectory planning. *Curr Opin Neurobiol* 9: 718–727, 1999.

Kawato M, Furukawa K, Suzuki R. A hierarchical neural-network model for control and learning of voluntary movement. *Biol Cybern* 57: 169–185, 1987.

Kawato M, Kuroda T, Imamizu H, Nakano E, Miyauchi S, Yoshioka T. Internal forward models in the cerebellum: fMRI study on grip force and load force coupling. *Prog Brain Res* 142: 171–188, 2003.

Kim CM, Eng JJ. Symmetry in vertical ground reaction force is accompanied by symmetry in temporal but not distance variables of gait in persons with stroke. *Gait Posture* 18: 23–28, 2003.

Kojima Y, Iwamoto Y, Yoshida K. Memory of learning facilitates saccadic adaptation in the monkey. *J Neurosci* 24: 7531–7539, 2004.

Krakauer JW, Pine ZM, Ghilardi MF, Ghez C. Learning of visuomotor transformations for vectorial planning of reaching trajectories. *J Neurosci* 20: 8916–8924, 2000.

Lee JY, Schweighofer N. Dual adaptation supports a parallel architecture of motor memory. *J Neurosci* 29: 10396–10404, 2009.

Maki BE, Holliday PJ, Topper AK. A prospective study of postural balance and risk of falling in an ambulatory and independent elderly population. *J Gerontol* 49: M72–M84, 1994.

Malone LA, Vasudevan EV, Bastian AJ. Motor adaptation training for faster relearning. *J Neurosci* 31: 15136–15143, 2011.

Mawase F, Karniel A. Evidence for predictive control in lifting series of virtual objects. *Exp Brain Res* 203: 447–452, 2010.

Mazzoni P, Krakauer JW. An implicit plan overrides an explicit strategy during visuomotor adaptation. *J Neurosci* 26: 3642–3645, 2006.

Medina JF, Garcia KS, Mauk MD. A mechanism for savings in the cerebellum. *J Neurosci* 21: 4081–4089, 2001.

Melzer I, Benjuya N, Kaplanski J. Age-related changes of postural control: effect of cognitive tasks. *Gerontology* 47: 189–194, 2001.

Morita S, Yamamoto H, Furuya K. Gait analysis of hemiplegic patients by measurement of ground reaction force. *Scand J Rehabil Med* 27: 37–42, 1995.

Morton SM, Bastian AJ. Cerebellar control of balance and locomotion. *Neuroscientist* 10: 247–259, 2004.

Morton SM, Bastian AJ. Cerebellar contributions to locomotor adaptations during splitbelt treadmill walking. *J Neurosci* 26: 9107–9116, 2006.

Munro CF, Miller DI, Fuglevand AJ. Ground reaction forces in running: a reexamination. *J Biomech* 20: 147–155, 1987.

Nichols DS. Balance retraining after stroke using force platform biofeedback. *Phys Ther* 77: 553–558, 1997.

Noble JW, Prentice SD. Adaptation to unilateral change in lower limb mechanical properties during human walking. *Exp Brain Res* 169: 482–495, 2006.

O'Connor SM, Kuo AD. Direction-dependent control of balance during walking and standing. *J Neurophysiol* 102:1411–1419, 2009.

Ohyama T, Mauk MD. Latent acquisition of timed responses in cerebellar cortex. *J Neurosci* 21: 682–690, 2001.

Önell A. The vertical ground reaction force for analysis of balance? *Gait Posture* 12: 7–13, 2000.

Peled A, Karniel A. Knowledge of performance is insufficient for implicit visuomotor rotation adaptation. *J Mot Behav* 44:185–194, 2012.

Perry J, Davids JR. Gait analysis: normal and pathological function. *J Pediatr Orthoped* 12: 815, 1992.

Reisman DS, Block HJ, Bastian AJ. Interlimb coordination during locomotion: what can be adapted and stored? *J Neurophysiol* 94: 2403–2415, 2005.

Reisman DS, Wityk R, Silver K, Bastian AJ. Locomotor adaptation on a split-belt treadmill can improve walking symmetry post-stroke. *Brain* 130: 1861–1872, 2007.

Roerdink M, Coolen B, Clairbois B, Lamoth CJ, Beek PJ. Online gait event detection using a large force platform embedded in a treadmill. *J Biomech* 41: 2628–2632, 2008.

Sakaguchi M, Taguchi K, Miyashita Y, Katsuno S. Changes with aging in head and center of foot pressure sway in children. *Int J Pediatr Otorhinolaryngol* 29: 101–109, 1994.

Scheidt RA, Reinkensmeyer DJ, Conditt MA, Rymer WZ, Mussa-Ivaldi FA. Persistence of motor adaptation during constrained, multi-joint, arm movements. *J Neurophysiol* 84: 853–862, 2000.

Shadmehr R, Mussa-Ivaldi FA. Adaptive representation of dynamics during learning of a motor task. *J Neurosci* 14: 3208, 1994.

Shadmehr R, Mussa-Ivaldi S. *Biological Learning and Control: How the Brain Builds Representations, Predicts Events, and Makes Decisions.* Cambridge, MA: MIT Press, 2012.

Smith MA, Ghazizadeh A, Shadmehr R. Interacting adaptive processes with different timescales underlie short-term motor learning. *PLoS Biol* 4: e179, 2006.

Smith MA, Shadmehr R. Intact ability to learn internal models of arm dynamics in Huntington's disease but not cerebellar degeneration. *J Neurophysiol* 93: 2809–2821, 2005.

Stubbs PW, Gervasio S. Motor adaptation following split-belt treadmill walking. *J Neurophysiol* 108: 1225–1227, 2012.

Tesio L, Rota V. Gait analysis on split-belt force treadmills: validation of an instrument. *Am J Phys Med Rehabil* 87: 515–526, 2008.

Thoroughman KA, Shadmehr R. Learning of action through adaptive combination of motor primitives. *Nature* 407: 742–747, 2000.

Tsaklis PV, Grooten WJ, Franzén E. Effects of weight-shift training on balance control and weight distribution in chronic stroke: a pilot study. *Top Stroke Rehabil* 19: 23–31, 2012.

Tseng Y, Diedrichsen J, Krakauer JW, Shadmehr R, Bastian AJ. Sensory prediction errors drive cerebellum-dependent adaptation of reaching. *J Neurophysiol* 98: 54–62, 2007.

Vasudevan EV, Bastian AJ. Split-belt treadmill adaptation shows different functional networks for fast and slow human walking. *J Neurophysiol* 103: 183–191, 2010.

White R, Agouris I, Selbie R, Kirkpatrick M. The variability of force platform data in normal and cerebral palsy gait. *Clin Biomech* 14: 185–192, 1999.

Winter DA. *Biomechanics and Motor Control of Human Gait: Normal, Elderly and Pathological.* Waterloo, ON, Canada: Univ. of Waterloo Press, 1991.

Wolpert DM, Ghahramani Z, Jordan MI. An internal model for sensorimotor integration. *Science* 269: 1880–1882, 1995.

Wolpert DM, Miall RC, Kawato M. Internal models in the cerebellum. *Trends Cogn Sci* 2: 338–347, 1998.

Woollacott MH, Shumway-Cook A. Postural dysfunction during standing and walking in children with cerebral palsy: what are the underlying problems and what new therapies might improve balance? *Neural Plast* 12: 211–219, 2005.

Yanagihara D, Kondo I. Nitric oxide plays a key role in adaptive control of locomotion in cat. *Proc Natl Acad Sci USA* 93: 13292–13297, 1996.

Yang JF, Lamont EV, Pang MY. Split-belt treadmill stepping in infants suggests autonomous pattern generators for the left and right leg in humans. *J Neurosci* 25: 6869–6876, 2005.